*34th EPS Conference on Plasma Phys. Warsaw, 2 - 6 July 2007 ECA Vol.**31F**, P-5.026 (2007)*

Simulations of β scan experiments using theory-based transport models

L Laborde, D C McDonald, I Voitsekhovitch and JET EFDA contributors*

EURATOM-UKAEA Fusion Association, Culham Science Centre, Abingdon, OX14 3DB, UK

Introduction

According to the similarity principle, transport can be described as a function of dimensionless parameters [1]. In particular, the β (kinetic to magnetic pressure ratio) dependence is of major importance for the estimation of performance in future thermonuclear devices. In a number of machines, dedicated scan experiments, where β is scanned while other dimensionless parameters are fixed, showed contrasting results: a strong degradation of confinement with increasing β has been reported in JT60-U and ASDEX-U [2, 3] while no dependence was seen in JET and DIII-D [4, 5]. Recently, a β degradation was observed in a JET high-shape hybrid-scenario [6].

In this paper, the β dependence of the theory-based models Multi-Mode (MMM95) [7] and GLF23 [8] is determined by running them stand-alone with imposed plasma profiles. The models are then used in predictive simulations of ion and electron temperatures in order to test the capability of the models to reproduce experimental scan results.

β dependence of MMM95 and GLF23 models

The 1995 version of the Multi-Mode model is used with the Weiland model as the only contribution to the turbulent transport: in contrast with [7], no additional model is used for kinetic and resistive ballooning modes. Growth rates and frequencies of Ion Temperature Gradient modes (ITG) and Trapped Electron Modes (TEM) are computed assuming a fixed poloidal wave vector (ITG/TEM range) and a MHD ballooning parameter α explicitly independent of β. The model includes effects from trapped electrons, impurity species, fast ions, $E \times B$ shear and finite beta (or elctromagnetic effects).

The retuned GLF23 model [8] computes turbulent mode growth rates and frequencies for ten poloidal wave numbers in the ITG/TEM range and ten for ETG. Effects of collisions, Landau damping, trapped electrons, impurity species, fast ions and $E \times B$ shear are included, as well as finite beta effects. In the $s-\alpha$ shifted circle equilibrium considered, α can be either fixed or varied consistently with β through $\alpha = -q^2 R_0 \frac{d\beta}{dr}$, where q is the safety factor, R_0 the major radius and r the minor radius. Both cases are tested here.

In both models, the $E \times B$ shear stabilization is implemented by introducing a net growth rate $\gamma_{net} = \gamma - \gamma_{E\times B}$ where γ is the instability growth rate and the $E \times B$ shear $\gamma_{E\times B}$ formula is taken from the GLF23 model [9].

The β dependence of the two models is investigated by performing the same β scan in the JET conditions used for recent dedicated experiments [6]: the discharge #68595 is used as a reference. The scan includes very high β values in order to show all the physics covered by the models; though this might not seem relevant regarding real fusion plasmas, some effects could appear at different β values with a small change in the scan parameters. In order to match dimensionless parameter profiles (normalized Larmor radius ρ^*, normalized collisionality ν^*, ion to electron temperature ratio T_i/T_e, safety factor q, magnetic shear s, toroidal Mach number M_{tor}, and effective charge Z_{eff}) while varying β ($\beta = 2\mu_0 \frac{k_B (n_e T_e + n_i T_i)}{B^2}$ where k_B is the Boltzmann's constant), imposed plasma parameters (plasma current I, ion and electron density

*See the Appendix of M L Watkins et al, Fusion Energy 2006 (Proc. 21st Int. Conf. Chengdu, 2006) IAEA, (2006).

n_i and n_e, ion and electron temperature T_i and T_e and toroidal rotation) must be scaled to different values of toroidal magnetic field B according to the following relations:

$$n_i \propto B^4, \qquad n_e \propto B^4, \qquad T_i \propto B^2, \qquad T_e \propto B^2, \qquad I \propto B, \qquad V_{tor} \propto B. \tag{1}$$

Figure 1 shows the variation of effective thermal diffusivity χ_{eff} ($\chi_{eff} = \dfrac{n_e\chi_e + n_i\chi_i}{n_e + n_i}$) and growth rates of most unstable modes in the ITG/TEM range at normalized toroidal radius $\rho = 0.4$, versus β. Normalizations from [1, 9] are used. Local values of the main normalized parameters are $q = 1.32$, $s = 0.71$, $\rho^* = 0.015$, $\nu^* = 0.06$. In figure 1a, it can be seen that MMM95 predicts the ITG stabilization, decribed in [10], up to a critical β value $\beta \approx 2\%$ corresponding to the onset of MHD ballooning modes. The GLF23 model physics underlying figure 1b is more complex. Three cases are studied. Full red traces are obtained keeping $\alpha = 0$ throughout the scan and including electromagnetic (EM) effects. In dash-dot magenta lines simulations, α is varied consistently with β ($\alpha = 0.1\beta$ with the above parameters), but EM effects are switched off. Dashed blue lines correspond to a scan where both effects are taken into account: α is varied consistently with β and EM effects are included. Note that it has been checked that a scan without EM effects and with constant α does not show any β dependence.

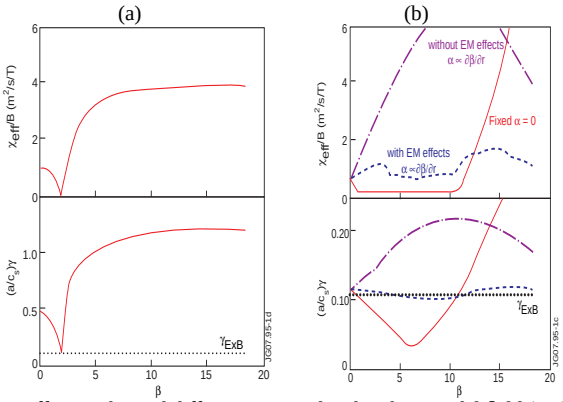

Fig. 1: Effective thermal diffusivity normalized to the toroidal field (top) and growth rates (bottom) of most unstable modes (ITG/TEM range only) as functions of β, for MMM95 ($\alpha = 0.3$ fixed) (a) and GLF23 (b) ($\alpha = 0$ fixed and EM effects included for full red traces, $\alpha = 0.1\beta$ (with the setup described in the text) and no EM effects for dash-dot magenta traces), $\alpha = 0.1\beta$ and EM effects included for dashed blue traces); black dotted line indicates $E \times B$ shear.

Looking at the full red traces, it can be seen that, as for MMM95, ITG modes are also stabilized by increasing β, with MHD ballooning modes appearing at $\beta \approx 6\%$. Though growth rates in ITG/TEM range only are plotted, diffusivities computed by the GLF23 model take into account the contribution from all unstable modes, including ETG modes which are not affected by $E \times B$ shear stabilization [11]. This is why the effective diffusivity given by the full red trace of figure 1b does not reach neoclassical values in the range $0.8\% \lessapprox \beta \lessapprox 11\%$ where ITG modes are fully stabilized by $E \times B$ shear: indeed, ETG modes, not represented on the figure, are still unstable and drive the turbulence. In contrast, MMM95 does not include ETG modes contribution; therefore, the transport in MMM95 is reduced to the neoclassical level as soon as ITG/TEM modes are stabilized by $E \times B$ shear.

When EM effects are switched off but α is consistent with β (dash-dot magenta traces), α is first destabilizing up to $\beta \approx 10\%$ where α-stabilization occurs. These opposite α effects are due to the low magnetic shear value ($s = 0.71$), as originally described in [8, 9].

Dashed blue lines show that, keeping α consistent with β and including EM effects, the destabilizing effect from α on both ITG and ETG is able to compensate toroidal ITG stabilization, as growth rates and diffusivity are then nearly constant; then, from $\beta \approx 10\%$, α-stabilization is in competition with ballooning modes, preventing the strong degradation seen on full red traces.

Predictive simulations of β scan

In order to test the capability of these models to reproduce the β dependence observed in experiments, time-dependent simulations are performed. Equilibrium, electron and ion temperature evolutions are predicted by the Astra transport code [12], taking experimental values

between $\rho = 0.8$ and $\rho = 1$ as boundary conditions. Transport coefficients taken from MMM95 and GLF23 (in GLF23, α is now consistent with β and EM effects are included) are added to neoclassical values to solve the heat transport equation. Simulated temperature profiles are initialized to experimental values and results are studied after several confinement times so that profiles can evolve according to the transport model. Geometric quantities, densities, toroidal velocity, effective charge, plasma current and power deposition profiles are taken from simulations with the Transp code [13].

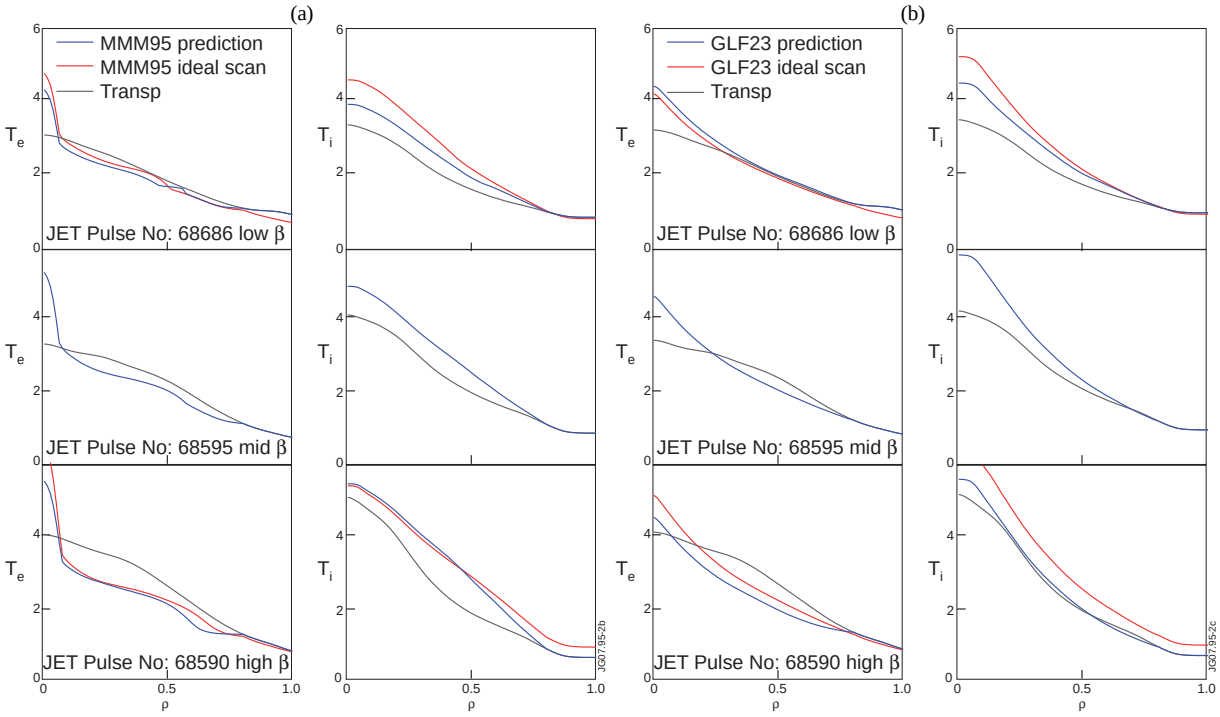

Fig. 2: Electron (left) and ion (right) temperature profiles from low (top) to high β_N (bottom) predicted by MMM95 (a) and GLF23 (b).

Three discharges are simulated, corresponding to a recent dedicated β scan experiment in JET where a strong β degradation was observed [6]. Analysis of this experiment is ongoing but the data shown here is indicative of the profiles matches seen in β scans. As we are interested in the global confinement dependence, the transport is now studied regarding a global value of β: $\beta_N = 100 \times 2\mu_0 \dfrac{p\,a}{B I_p}$ where p is the volume averaged plasma thermal pressure and a is the minor radius. In figure 2, blue traces show, for the three discharges from low (top) to high β_N (bottom), electron (left) and ion (right) temperature profiles predicted by MMM95 (a) and GLF23 (b). Profiles are averaged over a 0.5 s time window where dimensionless parameters (ρ^*, ν^*, T_i/T_e, q, s, M_{tor}, Z_{eff}) are best matched.

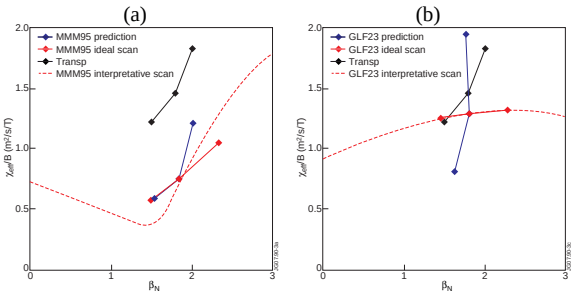

Fig. 3: Normalized diffusivity averaged over $0.3 \leq \rho \leq 0.7$ versus β_N for MMM95 (a) and GLF23 (b).

The β dependence emerging from these predicitve simulations must be taken with great care. Indeed, simulated profiles show a mismatch similar to the experimental one: some dimensionless parameter profiles differ by up to 20% from one run to another. This mismatch, especially on ρ^* and M_{tor} which have a strong impact on transport through gyroBohm scaling and $E \times B$

shear stabilization, leads to an apparent β dependence which differs from the one described in the previous section. Figure 3 shows the normalized diffusivity averaged over the gradient region $0.3 \leq \rho \leq 0.7$ as a function of β_N, for MMM95 (a) and GLF23 (b). The apparent β dependence deduced from this set of simulations, in blue, deviates, especially for the GLF23 model, from the red dashed line representing the first quarter of the ideal interpretative scan studied in figure 1: for instance, a slightly too high M_{tor} can increase $E \times B$ shear, reducing the transport and consequently the achieved β_N. In order to check that this deviation is due to the mismatch, another set of predictive simulations is performed. Taking inputs from the mid-β point, temperature boundary conditions, densities, power deposition profiles and toroidal rotation are adjusted, using relations (1), in order to match dimensionless parameters at the magnetic fields corresponding to low and high β_N discharges. The mid-β point simulation is left unchanged. The results from this ideal predicitive scan are plotted in red in figures 2 and 3. This time the observed dependence agrees well with results of the interpretative scan (dashed red traces): the degradation due to MHD ballooning modes appears in MMM95 (diffusivity scales as $\frac{\chi_{eff}}{B} \propto \beta_N^{1.3}$) while the different physical effects in competition in GLF23 lead to a very weak dependence ($\frac{\chi_{eff}}{B} \propto \beta_N^{0.1}$), to be compared with $\frac{\chi_{eff}}{B} \propto \beta_N^{1.0}$ or stronger observed in the experiment. It is worth mentioning that, though the trend with β observed in MMM95 seems to agree with the experiment, the experimental degradation may not be related to the ballooning modes as the critical β value is not precisely determined in MMM95.

Conclusion

The β dependence of the theory-based models MMM95 and GLF23 has been studied in the JET parametric conditions where a β degradation of confinement has been observed in experiment. MMM95 predicts a low critical β value for the onset of ballooning modes, leading to a loss of confinement with increasing β. In contrast, GLF23 predicts a critical β higher than the β experimental range; the inclusion of α effects and ETG modes in GLF23 can compensate ITG stabilization, leading to a weak β dependence. Though the inclusion of these effects is an improvement compared to the simpler physics of MMM95, a precise determination of the critical β value is a key point to improve these models. Predictive simulations have shown the sensitivity of those models, especially GLF23, to inexact matching of other dimensionless parameters.

This work was funded in part by the United Kingdom Engineering and Physical Sciences Research Council, by the European Communities under the contract of Association between EURATOM and UKAEA, and by a EURATOM Intra-European Fellowship.

References

[1] J W Connor *et al* 1977 *Nuclear Fusion* **17** 1047
[2] T Takizuka *et al* 2006 *Plasma Physics and Controlled Fusion* **48** 799
[3] L Vermare *et al* 2007 *Nuclear Fusion* **47** 490
[4] D C McDonald *et al* 2004 *Plasma Physics and Controlled Fusion* **46** A215
[5] C C Petty *et al* 2004 *Physics of Plasmas* **11** 2514
[6] D C McDonald in preparation for Plasma Physics and Controlled Fusion
[7] G Bateman *et al* 1998 *Physics of Plasmas* **5** 1793
[8] J E Kinsey *et al* 2005 *Physics of Plasmas* **12** 062302
[9] R E Waltz *et al* 1995 *Physics of Plasmas* **2** 2408
[10] J Weiland *et al* 1992 *Nuclear Fusion* **32** 151
[11] J E Kinsey *et al* 2002 *Physics of Plasmas* **9** 1676
[12] G Pereverzev *et al* 2002 Tech. Rep. 5/98 IPP-Report, Garching, Germany
[13] R J Goldston *et al* 1981 *Journal of computational physics* **43** 61